P161

CSEM Sensitivity Analysis Through Resolution Functions for Migration and Inversion

E.C. Slob* (Delft University of Technology) & W.A. Mulder (Shell International E&P BV)

SUMMARY

CSEM acquisition optimization is of interest to reduce acquisition costs, while maintaining the information content information in the data high. Fast methods for sensitivity analysis are useful to perform this task. We define a resolution function for migration and the resolution function for inversion to obtain an indication of s possible inversion result from acquired CSEM data. We model a conductivity perturbation in a conductive VTI lower half-space below a non-conductive lower half-space. We show that the resolution function for migration is capable of indicating the horizontal position of the perturbation, but not its depth. The introduced resolution function for inversion is shown to have a good horizontal and vertical resolution, where the horizontal resolution is virtually independent of the perturbation depth, while the vertical resolution decreases with increasing perturbation depth. In a VTI background medium, it seems that it is more important to accurately know the horizontal conductivity than it is to know vertical conductivity.

Introduction

For modeling and inversion of land and marine CSEM data for reservoir characterization and monitoring of hydrocarbon production, several studies have been carried out by, e.g. Druskin and Knizhnerman (1994); Commer and Newman (2004); Mulder (2006); Plessix *et al.* (2007); Lien and Mannseth (2008); Plessix and Mulder (2008); Black and Zhdanov (2009); Orange *et al.* (2009); Wirianto *et al.* (2010). Acquisition geometry related sensitivity analysis is of interest to optimize acquisition geometries. To find how a perturbation in the subsurface conductivity can be retrieved by inversion, a resolution function can be defined. The resolution function depends on the acquisition geometry, the frequency bandwidth, and the actual complexity of the subsurface conductivity distribution. The perturbation can be due to subsurface heterogeneity, or in the case of time-lapse electromagnetic monitoring, by time-lapse changes in the subsurface. Our goal is to demonstrate how a perturbation in the subsurface conductivity has an effect on the total data and show the sensitivity of the data of a simple scattering point located in homogeneous conductive half-space below a non-conductive half-space. We analyze the resolution function for this problem and define a resolution function for migration and a resolution function for inversion. We investigate how well a subsurface conductivity perturbation can be reconstructed from single component line data by analyzing a resolution function for migration using multi-frequency data, and with the aid of a resolution function for inversion applied to single frequency data.

Definition of the resolution function

Formally the Hessian of the corresponding least-squares problem defines the resolution function. The Hessian of three-dimensional problems presents a formidable computational effort that we cannot accomplish in reasonable amounts of time. We therefore select a tractable version of a model-driven resolution function that can be defined from the description of a scattering point buried in a conductive homogeneous half-space below a non-conductive half-space.

We take the background medium as two homogeneous half-spaces; an upper non-conductive half-space and a lower conductive half-space, with source and receivers located at the interface as a model for land CSEM. The solution for the electric field can be written in space-frequency domain as

$$E_k(x,\omega) = E_k^i(x,\omega) + \int_{x'\in\mathbb{D}^s} G_{kr}(x,x',\omega)\chi(x')E_r(x',\omega)\mathrm{d}x', \tag{1}$$

where E_k denotes the total electric field; E_k^i denotes the incident electric field, which is the field that exists in absence of the perturbation. The domain $\mathbb{D}^s$ is in principle the whole lower half-space where perturbations can occur. The Green function $G_{kr}(x,x',\omega)$ is the point-source response at location x' measured by a point-receiver at location x, in the two half-spaces configuration, while χ denotes the contrast function of the perturbations. For the resolution function it is sufficient to assume the perturbation is a point-perturbation and the integral is removed. The source of the field at the perturbation is x^s and the receiver is denoted x^r. Equation (1) is the rewritten for a perturbation at x^p as

$$E_{kr}(x^r,x^s,\omega) = E_{kr}^i(x^r,x^s,\omega) + G_{kj}(x^r,x^p,\omega)G_{rj}(x^s,x^p,\omega)R(x^p)I(\omega), \tag{2}$$

where source-receiver reciprocity has been used for the Green function containing the source coordinate, and the frequency dependent source current is denoted $I(\omega)$. Equation (2) is the data equation that models the data for a point scatterer in the lower half-space. The Green functions for an isotropic conductive lower half-space can be found in Raiche and Coggon (1975) and for a VTI conductive lower half-space in Slob *et al.* (2010). The scatter function of the point scatterer is given by $R(x^p)$.

To be able to reconstruct the scatter function we can use equation (2) as an equation for the unknown location x^p and unknown strength of the scatter function R

$$G_{kj}(x^r,x^i,\omega)G_{rj}(x^s,x^i,\omega)R(x^i)I(\omega) = E_{kr}(x^r,x^s,\omega) - E_{kr}^i(x^r,x^s,\omega), \tag{3}$$

which can be solved in the least-square error sense by matrix inversion for a number of possible image perturbation locations, x^i, in the lower half-space, depending on the number of source and receiver locations available in the data. To look at a practical in-line acquisition geometry with x-directed electric current sources ($r = 1$) and x-directed electric field receivers ($k = 1$) and assuming the scatter point is located in the x,z-plane below the acquisition line we can write the equation as

$$D(x^r,x^s;x^i,z^i,\omega)R(x^i,z^i) = E^s_{11}(x^r,x^s,\omega), \tag{4}$$

where the two-way diffusive field operator is given by

$$D(x^r,x^s;x^i,z^i,\omega) = G_{1r}(x^r,x^s,x^i,z^i,\omega)G_{1r}(x^r,x^s,x^i,z^i,\omega)I(\omega), \tag{5}$$

and the right-hand side of equation (4) is the scattered electric field, which is the response of the point scatterer in the two homogeneous half-spaces configuration. Because the right-hand side of equation (4) is the scattered field of the recorded data, being the response of the scatter point located at x^p, we can write it as

$$E^s_{11}(x^r,x^s,\omega) = G_{1r}(x^r,x^s,x^p,z^p,\omega)G_{1r}(x^r,x^s,x^p,z^p,\omega)I(\omega). \tag{6}$$

We can now define the resolution function as the resolution function for migration, R^{m}, for a fixed scattering point at x^p as

$$R^{\mathrm{m}}(x^i,x^p) = \sum_{x^r,x^s,\omega} W(x^r,x^s,\omega)D^*(x^r,x^s,x^i,z^i,\omega)G_{1r}(x^r,x^s,x^p,z^p,\omega)G_{1r}(x^r,x^s,x^p,z^p,\omega)I(\omega), \tag{7}$$

where the superscripted * denotes complex conjugation and W is a real weighting function that can remove the source and receiver effects in the data. We can also define the resolution function as the resolution function for inversion, R^{i}, for a fixed scattering point at x^p by casting equation (4) in matrix-vector form in the least-squares sense

$$\mathsf{M}(x,z;x^i,z^i)R(x^i,z^i) = \sum_{x^r,x^s,\omega} D^*(x^r,x^s,x,z,\omega)E_{11}(x^r,x^s,\omega), \tag{8}$$

where the range of the locations x,z is the same as for the possible image points of the perturbation, x^i,z^i, ensuring a square matrix, while the system matrix M is given by

$$\mathsf{M}(x,z;x^i,z^i) = \sum_{x^r,x^s,\omega} D^*(x^r,x^s,x,z,\omega)D(x^r,x^s,x^i,z^i,\omega). \tag{9}$$

This is not strictly a description of the Hessian, but a formulation of the scattering equation as a linear inverse problem for subsurface scatterers or time-lapse perturbations. The Hessian of the nonlinear least-squares inversion is the same as the Hessian for the linearized inverse problem (i.e. iterative migration with the Born approximation) if the Gauss-Newton approximation is used for the former. Let N denote the inverse of the system matrix M, then we can write the resolution function for inversion as

$$R^{\mathrm{i}}(x^i,x^p) = \sum_{x,z,\omega} \mathsf{N}(x,z;x^i,z^i) \sum_{x^r,x^s,\omega} D^*(x^r,x^s,x,z,\omega)E_{11}(x^r,x^s,\omega). \tag{10}$$

Because we have defined the resolution function only in the (x,z)-plane the inverse problem is not optimally defined and the inverse matrix N is only an approximation to inverse for the actual 3D problem. Both equations (7) and (10) are used in a numerical example to show the differences in the approaches.

Numerical example

We use a conductive half space characterized by a horizontal conductivity of $\sigma_h = 0.3$ S/m, and a vertical conductivity of $\sigma_v = 0.1$ S/m. There are 200 point sources located at the surface, each horizontally spaced by 20 m, while the 41 receivers are located at the surface and horizontally spaced by 250 m.

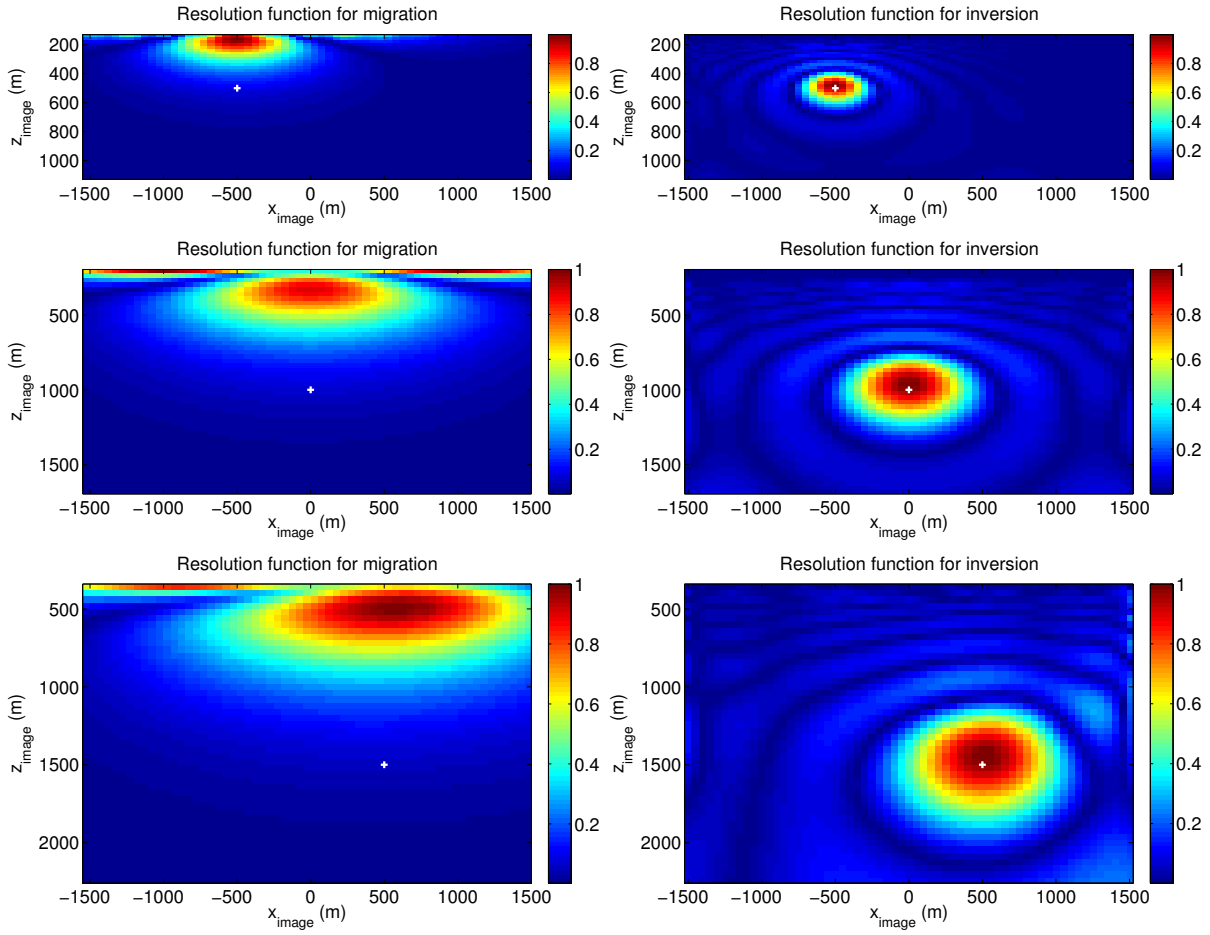

Figure 1 *Migration (left column) and inversion (right column) resolution function images for a scatter point at* $(x^p, z^p) = (-500, 500)$*,* $(x^p, z^p) = (0, 1000)$*, and* $(x^p, z^p) = (500, 1500)$*; in the images the white 'plus'-sign indicates the correct location of the scatter point.*

Relative to the midpoint of the source and receiver arrays, we have used three different scenarios for the scattering point. It is located at $(x^p, z^p) = (-500, 500)$, $(x^p, z^p) = (0, 1000)$, and $(x^p, z^p) = (500, 1500)$. For the example of the resolution function for migration we have used 11 frequencies equally spaced on a logarithmic scale between $f = 0.01$ Hz and $f = 10$ Hz. We have used the inverse of the incident field for each source and receiver position as weighting function to have some amplitude correction factor. For the examples for the resolution function for inversion we use a single frequency of $f = 0.5$ Hz. The (x, z)-plane we test for both resolution functions is $-1500 < x^i < 1500$ m and variable in depth depending on the depth of the scattering point.

Figure 1 shows the results for the migration (left-column) and inversion (right-column) resolution functions for the point scatterers at $(x^p, z^p) = (-500, 500)$ m (top row), $(x^p, z^p) = (0, 1000)$ m (middle row), and $(x^p, z^p) = (500, 1500)$ m (bottom row). For comparison the resolution functions have been normalized to their own maximum amplitudes in the image plane. From the left column it can be seen that the migration resolution function does not map the scatter point at the correct depth and the horizontal resolution decreases with the actual depth of the perturbation. From the right column of Figure 1 it can be seen that the horizontal location and depth are well retrieved in the resolution function for inversion. The inversion image maximum is located above the actual vertical position of the perturbation. This can be due to the fact that the maximum of the inversion image does not coincide with its center of gravity. The vertical resolution decreases with increasing depth, while the horizontal resolution is less sensitive to the depth of the perturbation than the migration resolution function. When the perturbation is deep and to the side of the acquisition line, some asymmetries occur in the inversion image.

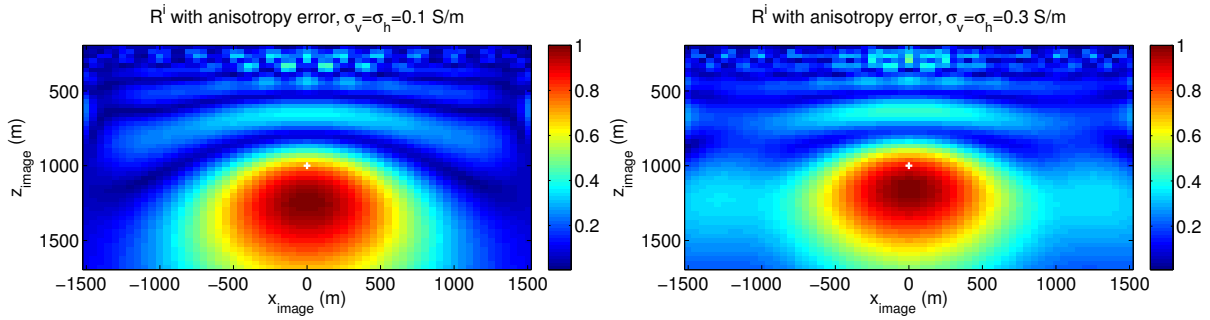

Figure 2 *Inversion resolution function images for a scatter point at* $(x^p, z^p) = (0, 1000)$ *for assuming the half-space is isotropic with vertical conductivity (left) and horizontal conductivity (right); in the images the white 'plus'-sign indicates the correct location of the scatter point.*

Figure 2 shows the inversion images when an error is made in the anisotropy. When we assume the conductivity to be the vertical conductivity, as shown in the left plot, the resolution is decreased and the maximum is lower than the actual location and when we assume the conductivity to be equal to the horizontal conductivity, as shown in the right plot, the vertical resolution is better than when we assume the conductivity to be the vertical conductivity, but the horizontal resolution is a little worse. It seems that it is more important to accurately know σ_h than it is to know σ_v.

Conclusions

For inversion of CSEM data sensitivity analysis is useful to assess the information content in the data based on a chosen acquisition geometry. We have described and analyzed an example of a conductivity perturbation in the subsurface of a simple model of two homogeneous half-spaces, where the lower half space is a VTI medium. We have shown how the resolution function for migration is capable of indicating the horizontal position of a conductivity perturbation, but not the vertical position, whereas the resolution function for inversion shows that even with single frequency, single component, line data the conductivity perturbation is properly located in horizontal position and depth. The horizontal resolution does not suffer much for deeper than for shallower perturbations, while the vertical resolution decreases with increasing depth of the perturbation. In an VTI background medium, it seems that it is more important to accurately know the background σ_h than it is to know σ_v.

References

Black, N., and Zhdanov, M. S. 2009. Monitoring of hydrocarbon reservoirs using marine CSEM method. *Pages 850–854 of: SEG Tech. Prog. Expanded Abstracts*.

Commer, M, and Newman, G. [2004] A parallel finite-difference approach for 3D transient electromagnetic modeling with galvanic sources. *Geophysics* 69(5), 1192–1202.

Druskin, V. I., and Knizhnerman, L. A. [1994] Spectral approach to solving three-dimensional maxwell's diffusion equations in the time and frequency domains. *Radio Science* 29(4), 937–953.

Lien, M., and Mannseth, T. [2008] Sensitivity study of marine csem data for reservoir production monitoring. *Geophysics* 73(4), F151–F163.

Mulder, W. A. [2006] A multigrid solver for 3D electromagnetic diffusion. *Geophysical Prospecting* 54(5), 633–649.

Orange, Arnold, Key, Kerry, and Constable, Steven. [2009] The feasibility of reservoir monitoring using time-lapse marine CSEM. *Geophysics* 74(2), F21–F29.

Plessix, R.-É., and Mulder, W. A. [2008] Resistivity imaging with controlled-source electromagnetic data: depth and data weighting. *Inverse Problems* 24(3), 034012.

Plessix, R.-É., Darnet, M., and Mulder, W. A. [2007] An approach for 3D multisource, multifrequency CSEM modeling. *Geophysics* 72(5), SM177–SM184.

Raiche, A. P., and Coggon, J. H. [1975] Analytic Greens tensors for intergal-equation modeling. *Geophysical Journal of the Royal Astronomical Society* 42(3), 1035–1038.

Slob, E., Hunziker, J., and Mulder, W. A. [2010] Green's tensors for the diffusive electric field in a VTI half-space. *Progress in Electromagnetics Research-PIER* 107, 1–20.

Wirianto, M., Mulder, W. A., and Slob, E. C. [2010] A feasibility study of land CSEM reservoir monitoring in a complex 3-D model. *Geophysical Journal International* 181(2), 741–755.